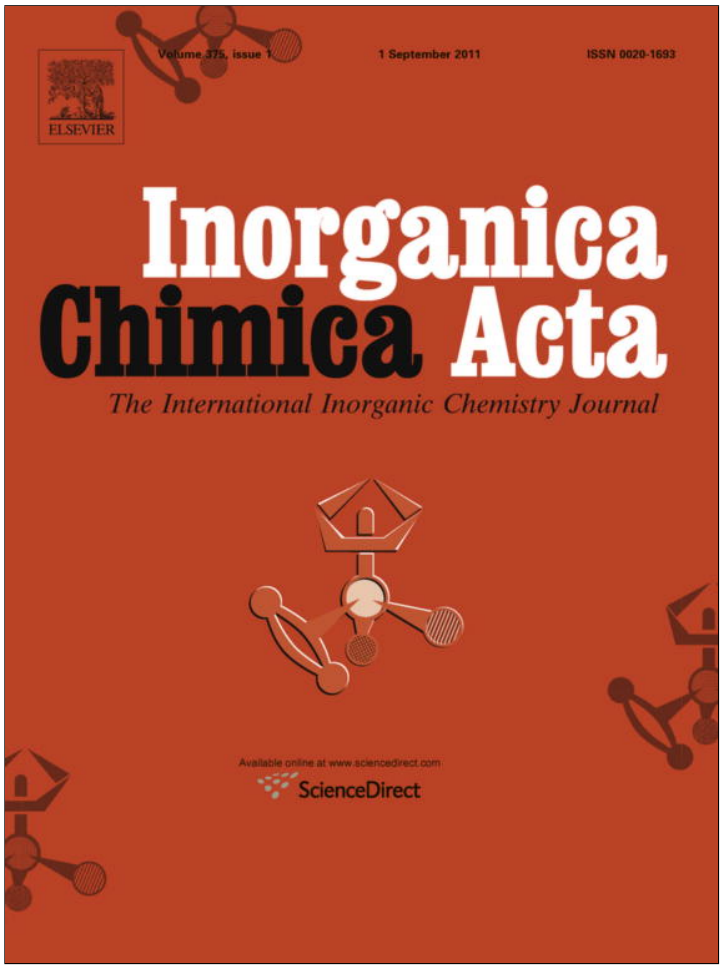

Inorganica Chimica Acta 375 (2011) 114–121

Contents lists available at ScienceDirect

Inorganica Chimica Acta

journal homepage: www.elsevier.com/locate/ica

Synthesis, structural characterization and biological studies of novel mixed ligand Ag(I) complexes with triphenylphosphine and aspirin or salicylic acid

M. Poyraz [a,1], C.N. Banti [a,h], N. Kourkoumelis [b], V. Dokorou [a,c], M.J. Manos [d], M. Simčič [e], S. Golič-Grdadolnik [f], T. Mavromoustakos [g], A.D. Giannoulis [a], I.I. Verginadis [h], K. Charalabopoulos [h], S.K. Hadjikakou [a,*]

[a] Inorganic and Analytical Chemistry, Department of Chemistry, University of Ioannina, 45110 Ioannina, Greece
[b] Medical Physics Laboratory, Medical School, University of Ioannina, 45110 Ioannina, Greece
[c] X-Ray Unit, Department of Chemistry, University of Ioannina, 45110 Ioannina, Greece
[d] Department of Chemistry, University of Cyprus, 1678 Nicosia, Cyprus
[e] Laboratory of Biomolecular Structure, National Institute of Chemistry, Hajdrihova 19, SI-1001 Ljubljana, Slovenia
[f] EN-FIST Centre of Excellence, Dunajska 156, SI-1000 Ljubljana, Slovenia
[g] Organic Chemistry Laboratory, Department of Chemistry, University of Athens, Greece
[h] Department of Experimental Physiology, Medical School, University of Ioannina, 45110 Ioannina, Greece

ARTICLE INFO

Article history:
Received 21 January 2011
Received in revised form 16 April 2011
Accepted 20 April 2011
Available online 5 May 2011

Keywords:
Bioinorganic chemistry
Silver(I) complexes
Aspirin
Crystal structures
Cytotoxic activity
STD ^{1}H NMR

ABSTRACT

Two new mixed ligand silver(I) complexes of formulae {[Ag(tpp)$_3$(asp)](dmf)} (**1**) (aspH = o-acetylsalicylic acid and tpp = triphenylphosphine) and [Ag(tpp)$_2$(o-Hbza)] (**2**) (o-HbzaH = o-hydroxy-benzoic acid) were synthesized and characterized by elemental analyses, spectroscopic techniques and X-ray crystallography at ambient conditions. Three phosphorus and one carboxylic oxygen atoms from a de-protonated aspirin ligand in complex **1** and two phosphorus and two carboxylic oxygen atoms from a chelating o-Hbza anion in complex **2** form a tetrahedral geometry around Ag(I) ions in both complexes.

Complexes **1** and **2** and the silver(I) nitrate, tpp, aspNa and o-HbzaH were tested for their *in vitro* cytotoxic activity against leiomyosarcoma cells (LMS), human breast adenocarcinoma cells (MCF-7) and normal human fetal lung fibroblasts (MRC-5) cells with Thiazolyl Blue Tetrazolium Bromide (MTT) assay. For both cell lines **1** and **2** were found to be more active than cisplatin. Additionally, **1** and **2** exhibit lower activity on cell growth proliferation of MRC-5 cells. The type of LMS cell death caused by **1** and **2** were evaluated *in vitro* by use of flow cytometry assay. The results show that at concentrations of 1.5 and 1.9 μM of complex **1**, 44.1% and 69.4%, respectively of LMS cells undergo programmed cell death (apoptosis). When LMS cells were treated with 1.6 and 2.3 μM of **2**, LMS cells death was by 29.6% and 81.3%, respectively apoptotic. Finally, the influence of the complexes **1** and **2**, upon the catalytic peroxidation of linoleic acid to hydroperoxylinoleic acid by the enzyme lipoxygenase (LOX) was kinetically and theoretically studied. The binding of **1** and **2** towards LOX was also investigated by Saturation Transfer Difference (STD) ^{1}H NMR experiments.

1. Introduction

Aspirin (aspH) (o-acetyl-salicylic acid) was the first member of the class of drugs known as nonsteroidal, anti-inflammatory drugs (NSAIDs) discovered. Aspirin was introduced as an anti-pyretic, anti-inflammatory and analgesic drug at the end of nineteenth century, while today, is one of the most commonly drug in use, worldwide [1]. A number of epidemiological studies have indicated that long term aspirin/NSAID use is associated with 30–50% reduction in risk of colorectal cancer or adenomatous polyps or death from colorectal cancer [2a]. Other epidemiologic studies also found associations between aspirin/NSAID use and a lower death rate from cancers of the esophagus, stomach, breast, lung, prostate, urinary bladder and ovary [2b,c]. Salicylic acid (o-HbzaH) (o-hydroxybenzoic acid), is a precursor of aspirin, while it has been recently shown that organotin complexes of o-HbzaH possess strong antiproliferative activity [3]. The biomedical applications and uses of silver(I) complexes, on the other hand, are related to their antibacterial action [1b,4] which appears to involve interaction with DNA [4,5]. Recently, Ag(I) complexes have also been studied for their antitumor activity [5,6]. Despite the importance of aspirin only few structures of complexes are available up to now. These include the complexes of aspirin with calcium(II) [7a], copper(II) [7b–d], nickel(II) [7e], tin(IV) [7f], cadmium(II) [7g], zinc(II) [7h]. The silver(I) complex of salicylic acid, however, with formula {[Ag(o-Hbza)]$_2$} is already known [8].

* Corresponding author. Tel.: +30 26510 08374; fax: +30 26510 08786.
E-mail address: shadjika@uoi.gr (S.K. Hadjikakou).
[1] On leave from Chemistry Department, Afyon Kocatepe University, Turkey

0020-1693/$ - see front matter © 2011 Elsevier B.V. All rights reserved.
doi:10.1016/j.ica.2011.04.032

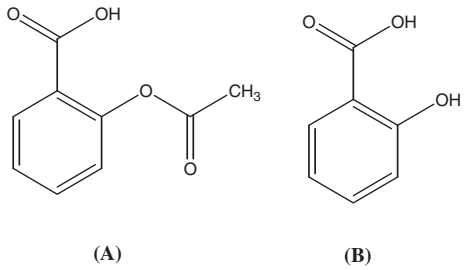

(A) (B)

Scheme 1. Molecular formulae of aspH (A) and o-HbzaH (B).

Lipoxygenase (LOX) is an enzyme which catalyzes the oxidation of arachidonic acid to leukotrienes, in an essential mechanism for the cell life involving in inflammation mechanism [9a,b]. LOX inhibition is found to induce apoptosis [9c], while the lipid peroxides derived from fatty acids metabolism by LOX can regulate cellular proliferation [9d]. Thus, LOX inhibition provides a potential novel target for the treatment and chemoprevention for a number of different cancers.

In the course of our studies on metallotherapeutics [10], we have synthesized new silver(I) complexes of formulae {[Ag(tpp)$_3$(asp)](dmf)} (**1**) (aspH = o-acetylsalicylic acid (Scheme 1A) and tpp = triphenylphosphine) and [Ag(tpp)$_2$(o-Hbza)] (**2**) (o-HbzaH = o-hydroxy-benzoic acid (Scheme 1B). The complexes were characterized by elemental analyses, spectroscopic techniques and X-ray crystallography at ambient conditions. The anti-cancer cell screening results against LMS and MCF-7 showed that both complexes **1** and **2** are more active than cisplatin and less active against MRC-5 cells proliferation. These findings are compared with the results of the influence of **1** and **2**, on the catalytic peroxidation of linoleic acid to hydroperoxylinoleic acid by the enzyme LOX.

2. Results and discussion

2.1. General aspects

Crystals of the complexes **1** and **2** have been grown as follows: $AgNO_3$ reacts with the sodium salts of aspirin or o-hydroxy-benzoic and white precipitations are formed. Slow evaporation of DMF solutions of these precipitations in the presence of triphenylphosphine give crystals of **1** and **2**. The formula of the complexes was firstly deduced from its elemental analysis, m.p. and their spectroscopic data (see Section 4). The X-ray crystal structures of complexes were also determined. The crystals of the complexes are air stable when they store in darkness at room temperature. Complexes **1** and **2** are soluble in MeCN, $CHCl_3$, CH_2Cl_2 DMSO, DMF and CH_3OH. Since a dissociation of the Ag–P bonds have been observed for silver(I) complexes with phosphines and carboxylic acids in solution [11], the stability of the complexes **1** and **2** in DMSO solutions were tested by UV–Vis spectra and conductivity measurements. No any changes were observed between the initial UV spectrum and the corresponding one measured after 48 h for both complexes (Fig. S1). The period of 48 h for the stability testing of the complexes was chosen since biological experiments require 48 h of incubation with complexes. In order to assure that no any ionic species are also formed in DMSO or DMSO/water solutions, the molar conductance (Λ_m) values of the complexes **1** and **2** in DMSO solution (10^{-3} M) were determined (**1**: 15.0 (0 h), 15.2 (48 h), 15.0 (72 h) and **2**: 17.8 (0 h), 18.1 (48 h), 14.4 (72 h) Ω^{-1} cm^2 mol^{-1}). These values showed that the solutions of the complexes are not conducting, confirming their stability in DMSO or DMSO/water media. The molar conductance of the silver(I) nitrate complex with tetramethylethylenediamine [Ag((CH$_3$)$_2$NCH$_2$CH$_2$N(CH$_3$)$_2$)]NO$_3$ was 40 Ω^{-1} cm^2 mol^{-1}, in excellent agreement with values for fully dissociated 1:1 electrolytes, such as sodium nitrate, in DMSO [11b]. The corresponding molar conductivity of DMSO solutions, measured for the ionic AgX salts (X = NO_3^-, BF_4^-) with (1-benzyl-2-imidazolyl)diphenylphosphine [(Bzlm)Ph$_2$P] are 302 and 320 Ω^{-1} cm^2 mol^{-1} [11c] indicating the formation of three ionic species in DMSO solution.

Attempts for the preparation of the initial sample by reacting $AgNO_3$ and aspirin in aqueous NH_3 40% solution lead to the formation of the [Ag(o-Hbza)]$_2$ (**3**) complex, where a hydrolysis of the ester (aspirin) to its o-HbzaH processor has been occurred. The crystal structure of **3** was also determined (crystallized in $P2_1/c$ with a = 7.3973(2), b = 8.6899(2), c = 10.5388(3) Å, β = 107.2560(10)°) and is almost identical with those reported earlier [8a] ($P2_1/c$, a = 7.405(1), b = 8.826(2), c = 10.683(2) Å, b = 107.48(4)°).

2.2. Crystal and molecular structures of {[Ag(tpp)$_3$(asp)](dmf)} (1) and [Ag(tpp)$_2$(o-Hbza)] (2)

ORTEP diagrams of **1** and **2** along with their selected bond distances and angles are shown in Figs. 1 and 2.

In case of **1**, three phosphorus atoms from tpp ligands and one deprotonated carboxylic oxygen atom from aspirin form a tetrahedral geometry around Ag(I) ion. Two phosphorus atoms from tpp and two oxygen atoms from the deprotonated carboxylic group which chelates Ag(I) ion form the tetrahedral geometry around silver(I) in case of **2**. The average Ag–P bond distance in **1** is 2.53 Å (Ag1–P1 = 2.515(2), Ag1–P2 = 2.554(3), Ag1–P3 = 2.528(3)), while in **2** is 2.43 (Ag(1)–P(1) = 2.4030(6), Ag(1)–P(2) = 2.4589(7)). The corresponding bond distances observed in silver(I) mixed ligand complexes of phosphines and carboxylic acids are: 2.6026(8), 2.5441(7) and 2.5432(7) Å in (Ph$_3$P)$_3$AgOC(O)C$_2$F$_5$ [12a], 2.543(2), 2.563(2) and 2.546(3) Å in [Ag(2-sbaH)(PPh$_3$)$_3$] (2-sbaH$_2$ = 2-sulfobenzoic acid) [12b], 2.524(7), 2.545(8) and 2.503(8) Å in [Ag(dppe)(tfa)]$_n$ (dppe = diphenyl-phosphinethane, tfa = F$_3$CCO$_2$) [12c], 2.365(2) and 2.344(2) Å in [Ag$_2$(CH$_3$CO$_2$)$_2$(dppf)]$_2$ (dppf =

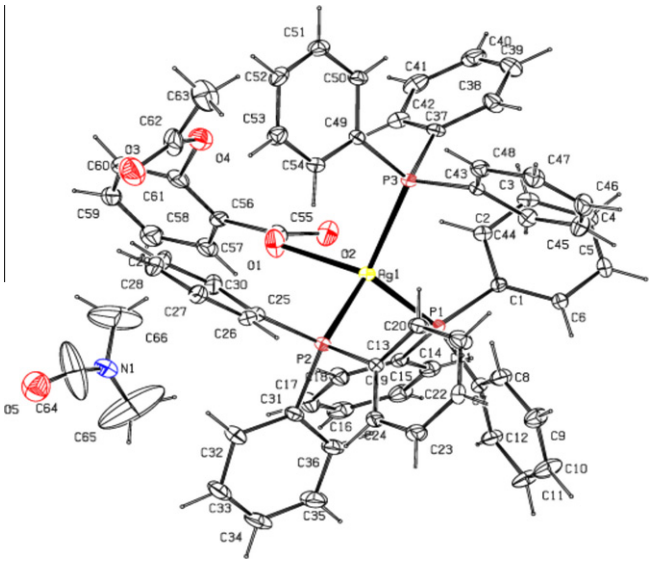

Fig. 1. ORTEP diagram together with labeling scheme of **1**. Thermal ellipsoids drawn at the 50% probability level. Selected bond lengths (Å) and angles [°]: Ag1–P1 = 2.515(2), Ag1–P2 = 2.554(3), Ag1–P3 = 2.528(3), Ag1–O1 = 2.395(10), O1–C55 = 1.144(18), O2–C55 = 1.287(17), O3–C62 = 1.16(2), O4–C61 = 1.388(17), O4–C62 = 1.303(18), P1–Ag1–P2 = 109.32(9), P1–Ag1–P3 = 115.37(8), P1–Ag1–O1 = 110.4(2), P2–Ag1–P3 = 117.09(8), P2–Ag1–O1 = 101.4(2),P3–Ag1–O1 = 101.9(3); solvated DMF: O5–C64 = 1.07(3), N1–C64 = 1.21(3).

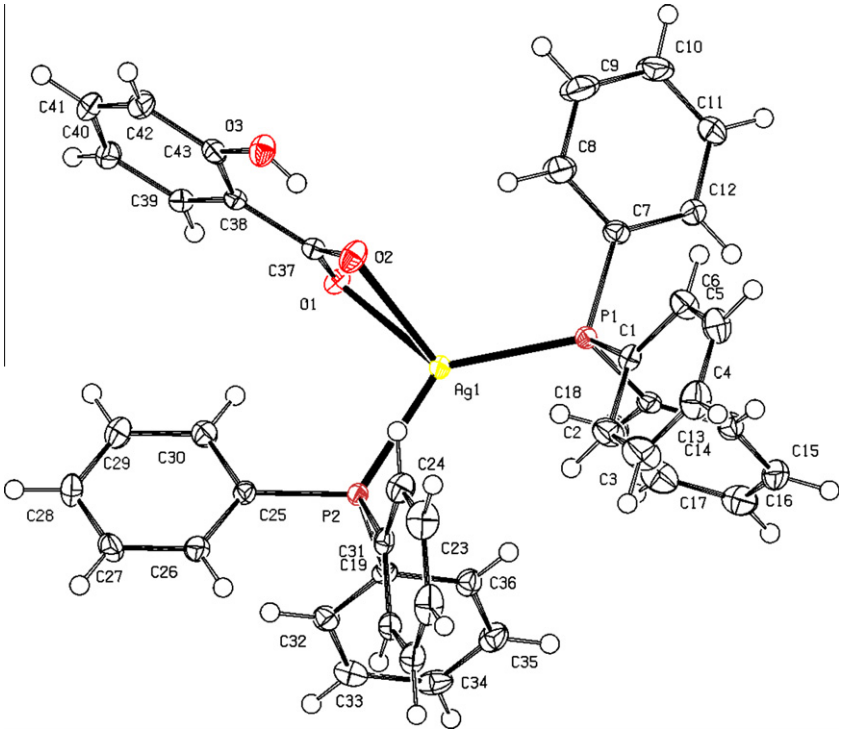

Fig. 2. ORTEP diagram together with labeling scheme of **2**. Thermal ellipsoids drawn at the 50% probability level. Selected bond lengths (Å) and angles [°]: Ag(1)–P(1) = 2.4030(6), Ag(1)–P(2) = 2.4589(7), Ag(1)–O(1) = 2.4045(12), Ag(1)–O(2) = 2.5230(12), O(1)–C(37) = 1.2535(17), O(2)–C(37) = 1.2752(18), O(3)–C(43) = 1.3539(19), O(3)–HA = 0.7768, P(1)–Ag(1)–O(1) = 125.49(3), O(1)–Ag(1)–P(2) = 99.22(3), P(1)–Ag(1)–P(2) = 133.358(16), , P(1)–Ag(1)–O(2) = 112.55(3), P(2)–Ag(1)–O(2) = 104.02(3), O(1)–Ag(1)–O(2) = 53.57(4).

1,l′-bis(dipheny1-phosphino) ferrocene) [12d], 2.340(4) and 2.364(5) Å in $[Ag_2(C_6H_5CO_2)_2(dppf)]$ [12d], 2.523(5), 2.544(5), 2.496(5) Å in $[Ag_2(HCO_2)_2(dppf)_3]$ [12d], 2.5199(7), 2.5237(6), 2.4953(7) Å in $[Ag(PPh_3)_3O_2CH]HCO_2H$ [12e], 2.527(2), 2.533(2), 2.510(3) Å in $[Ag(PPh_3)_3O_2CH]$ [12e], 2.482, 2.508, 2.439, Å in $[Ag(dppe)_3(CF_3COO)]_2$ (dpph = 1,6-bis(diphenyl-phosphino) hexane) [12f]. The Ag–O bond distance in **1** is 2.395(10) Å and in **2** are 2.4045(12) and 2.5230(12) Å, while the corresponding bond distances measured are: 2.433(2) Å in $(Ph_3P)_3AgOC(O)C_2F_5$ [12a], 2.559(11) Å in $[Ag(2\text{-}sbaH)(PPh_3)_3]$ (2-sbaH$_2$ = 2-sulfobenzoic acid) [12b], 2.499(1) Å in $[Ag(dppe)(tfa)]_n$ (dppe = diphenyl-phosphinethane, tfa = F_3CCO_2) [12c], 2.268(2) Å in $[Ag_2(CH_3CO_2)_2(dppf)]_2$ (dppf = 1,l′-bis(dipheny1-phosphino) ferrocene) [12d], 2.219(9) Å in $[Ag_2(C_6H_5CO_2)_2(dppf)]$ [12d], 2.65(2) Å in $[Ag_2(HCO_2)_2(dppf)_3]$ [12d], 2.5199(7), 2.509(2) Å in $[Ag(PPh_3)_3O_2CH]HCO_2H$ [12e], 2.507(9) Å in $[Ag(PPh_3)_3O_2CH]$ [12e].

The Ag···$O_{carboxylic}$ in 1 distance is 3.248 Å which is shorter than the sum of van der Waals radius of silver and oxygen (3.65–4.08 Å) [13]. However, this distance could not be considered as bonding interaction since the geometry around the metal center is tetrahedron as the bond angles varied between 101.4(2)° and 117.09(8)° (Fig. 1), whereas bonding interaction should lead to square pyramidal arraignment with bond angle around 90°. The close Ag···$O_{carboxylic}$ distance is explained to the steric effect caused to the sp^2 hybridism of the carboxylic carbon which is also bonded to the carboxylic oxygen donor atom. The corresponding carbonylic oxygen-silver distances observed are: 3.413 Å in $(Ph_3P)_3AgOC(O)C_2F_5$ [12a], 3.425 Å in $[Ag(2\text{-}sbaH)(PPh_3)_3]$ (2-sbaH$_2$ = 2-sulfobenzoic acid) [12b], 3.094 Å in $[Ag(dppe)(tfa)]_n$ (dppe = diphenyl-phosphinethane, tfa = F_3CCO_2) [12c], 3.116 Å in $[Ag_2(HCO_2)_2(dppf)_3]$ [12d] and they are all ascribed as non bonding interactions [12]. The Ag–O bond distances in **2** are Ag1–O978 = 2.5230, Ag1–O987 = 2.4043 indicating the chelation of carboxylic group to silver(I) ions.

2.3. Biological tests

2.3.1. Cytotoxicity

Complexes **1** and **2**, were tested for their *in vitro* cytotoxic activity against leiomyosarcoma cancer cells (LMS) (mesenchymal tissue) from the Wistar rat, polycyclic aromatic hydrocarbons (PAH, benzo[a]pyrene) carcinogenesis, human breast adenocarcinoma cells (MCF-7) and normal human fetal lung fibroblasts (MRC-5) cells. The cell growth proliferation activities were evaluated with Thiazolyl Blue Tetrazolium Bromide (MTT) assay. The IC_{50} values of the complexes and their ligands against the cell lines tested are summarized in Table 1. The final IC_{50} values for cell growth proliferation after 48 h incubation with **1** and **2** against LMS cells are: 1.5 ± 0.1 and 1.6 ± 0.3 μM, respectively, while against MCF-7 cells are: 1.6 ± 0.2 and 2.5 ± 0.5 μM, respectively. The cell growth proliferation activity of cisplatin against LMS cells, evaluated by

Table 1
IC_{50} values of the complexes and their ligands against the cell lines tested.

Compounds	IC_{50} (μM)			References
	LMS	MCF-7	MRC-5	
1	1.5 ± 0.1	1.6 ± 0.2	2.9 ± 0.1	*
2	1.6 ± 0.3	2.5 ± 0.5	3.1 ± 0.3	*
$AgNO_3$	3.7 ± 0.3	3.3 ± 0.2	27.7 ± 3.3	*
AspNa	>350	>350	>350	*
o-HbzaH	>400	>400	>400	*
tpp	67.4 ± 13.9	56.5 ± 10.6	>160	*
$[AgCl(tptp)_3]$ (0.5 H_2O)	0.8 ± 0.08			[5]
$[AgI(tptp)_3]$	1.5 ± 0.06			[5]
$[AgCl(cmbzt)(tptp)_2]$	8 ± 0.39			[5]
Cisplatin	25	20	–	[10a,14a]

* This work.

MTT assay, was found to be 25 μM [10a], while against MCF-7 evaluated with the same assay, is given equal to 20 μM [14a]. Thus, both complexes **1** and **2** were found to exhibit significant higher activity (10-fold) than that of cisplatin against LMS and MCF-7 cells. Also, complexes **1** and **2** also show significantly stronger activity than their ligands (tpp, aspNa and o-HbzaH) (Table 1) and stronger activity (2-fold) than that of silver(I) nitrate (a known antimicrobial agent [1b]). Additionally, **1** and **2** was found to exhibit lower activity on cell growth proliferation of MRC-5 cells (normal human fetal lung fibroblast) with IC_{50} values 2.9 ± 0.1 and 3.1 ± 0.3 μM, respectively.

2.3.2. Flow cytometry

A flow cytometry assay was used to quantify apoptotic or necrotic cells, treated with compounds **1** and **2**. Treated and untreated LMS cells were stained with Annexin V-FITC and Propidium Iodide (PI). Fig. 3, shows the dose-dependent cytotoxic response in LMS cells through apoptosis when treated with **1**. Compared to untreated LMS cells which showed a total of 15.2% of background cells death (10.4% apoptosis and 4.8% necrosis), the cells treated with complex **1** (1.5 μM) showed 44.1% apoptosis (early apoptotic cells (Ann+/PI−) and late apoptotic cells (Ann+/PI+)) and 8.8% necrosis. When LMS cells were treated with 1.9 μM of **1**, 69.4% of the cells were early and late apoptotic and 8.9% necrotic. LMS cells treated with the complex **2** (1.6 μM), show 29.6% apoptosis (early and late apoptotic cells) and 5.0% necrosis, while when LMS cells were treated with 2.3 μM of 2, 81.3% of the cells were early and late apoptotic and 1.6% of the cells undergo necrosis. In this case the untreated LMS cells show a total of 10.5% of background cells death (7.9% apoptosis and 2.6% necrosis). Thus, complex **1** and **2** cause a dose dependent cytotoxic response in LMS cells through apoptosis. Although, no direct comparison can be made due to the different cell lines used, the apoptosis of HeLa cells induced by 33.75 μM solution of organogold(III) complexes containing the "pincer" iminophosphorane ligand (2-C_6H_4-PPh_2 = NPh) of formula [Au{κ^2-C,N-C_6H_4(PPh_2 = N(C_6H_5)-2}Cl2] is 23.3% [14b].

*2.4. Study of the peroxidation of linoleic acid by the enzyme lipoxygenase in the presence of complexes **1** and **2** and their ligands*

Since LOX inhibition is found to induce apoptosis [9c] the influence of complexes 1 and 2 on the oxidation of linoleic acid by the enzyme LOX were studied in a wide concentration range. The degree of LOX activity (A, %) in the presence of these complexes was calculated according to the method described previously [15]. Fig. 4 compares the inhibitory effect of **1**, **2** and cisplatin in various concentrations The IC_{50} values found for complexes are 7.2 (**1**), 2.3 (**2**) and 65.9 (cisplatin) μM, respectively. Thus, both complexes exhibit significantly higher inhibitory activity of LOX than cisplatin. LOX inhibition activity is found to be related to the cytotoxic activity against LMS cells [10]. Therefore, the high cytostatic activity caused by **1** and **2** (see above) might be attributed to their LOX inhibitory activity.

The binding of **1** and **2** towards LOX was also investigated by STD ^{1}H NMR experiment. On the top of Fig. 5A and B the aromatic region of the off-resonance NMR spectra are shown and on the bottom the on-resonance STD ^{1}H NMR spectra of the complexes **1** and **2**. Peaks attributed to the aspirin or o-hydroxy-benzoic acid molecules *ca* 6.9, 7.4–7.5 ppm and 7.8 ppm and peaks attributed to triphenylphosphine *ca* 7.6–7.7 ppm of the complexes **1** and **2** are

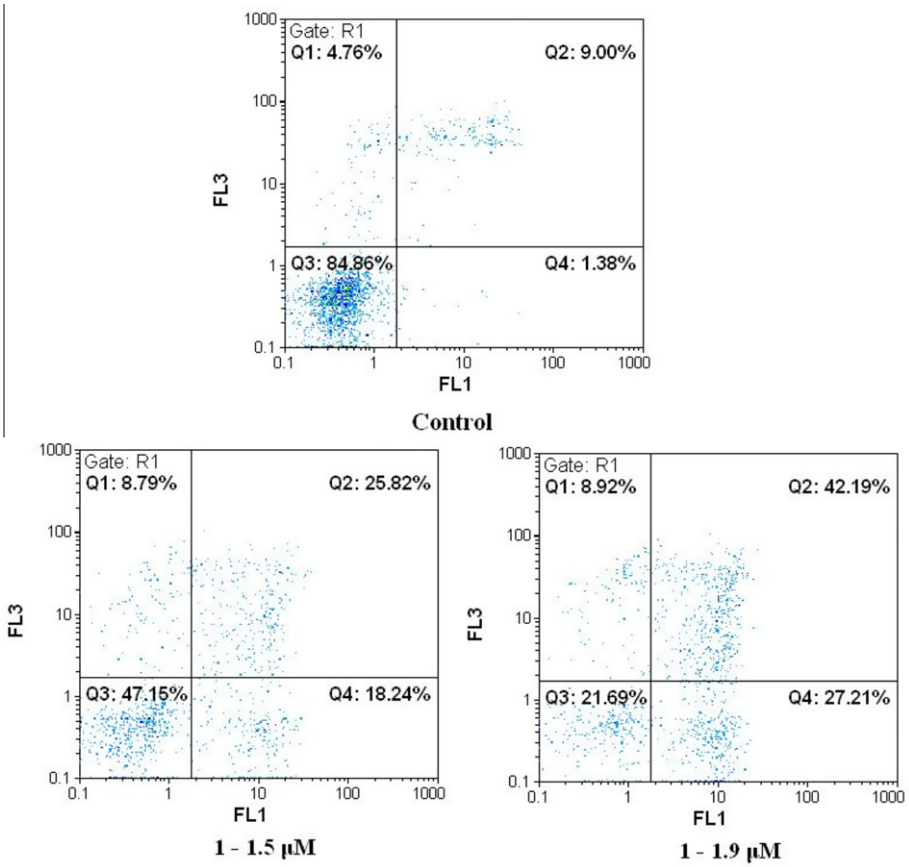

Fig. 3. Flow cytometry assay summary results for LMS cells, treated with various concentrations of **1** (1.5 and 1.9 μM) for 48 h of incubation, in comparison with the untreated cells (control).

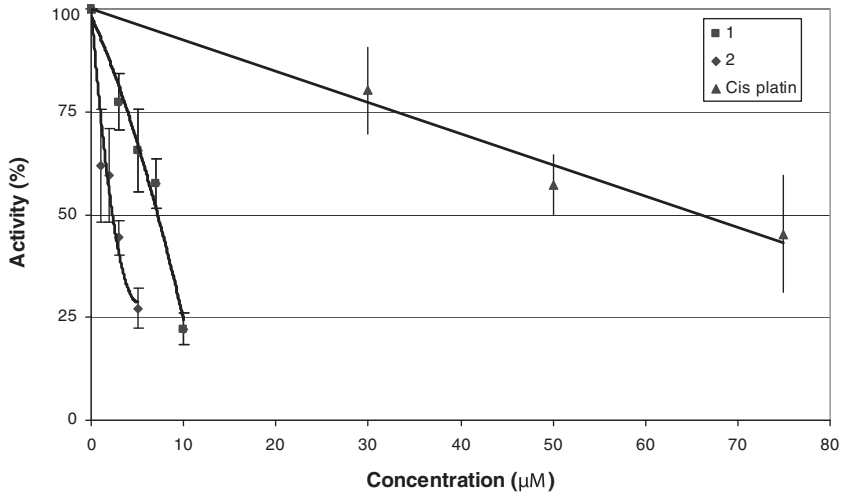

Fig. 4. The inhibitory effect against LOX caused by **1**, **2** and cisplatin in various concentrations.

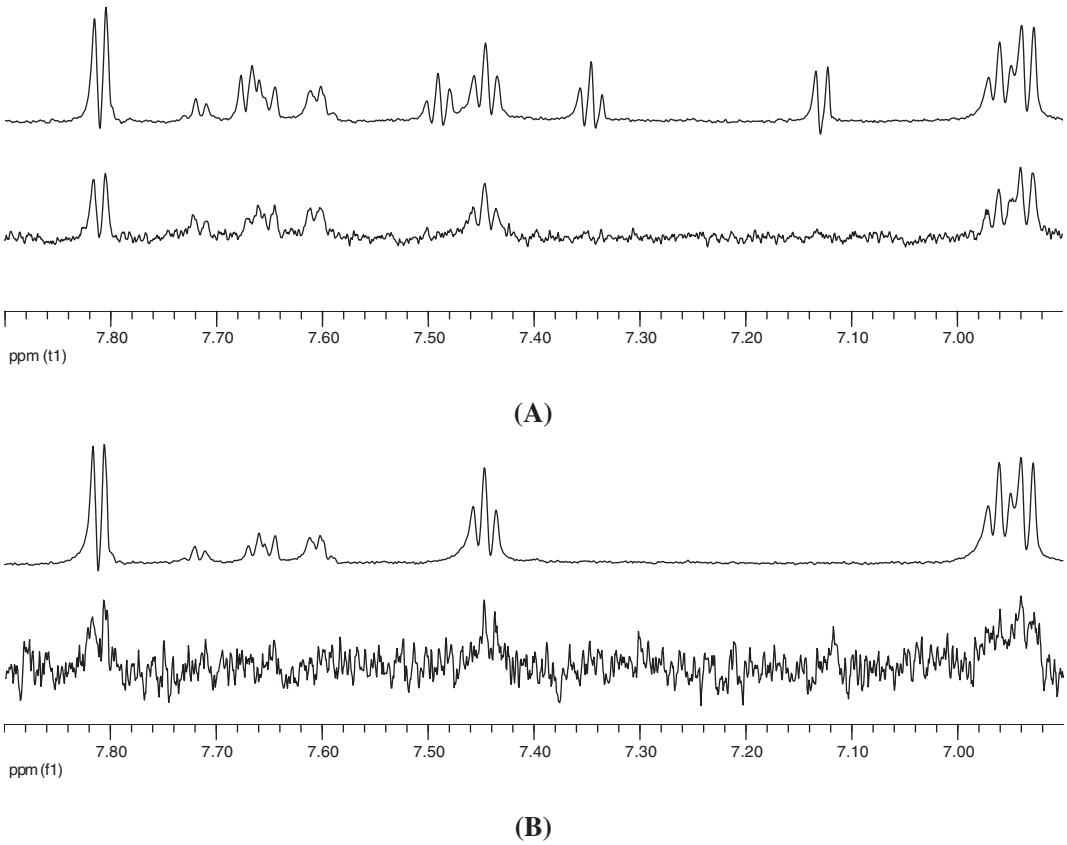

Fig. 5. The off-resonance reference NMR spectrum (top) and the on-resonance STD NMR spectrum (bottom) for the 1-protein (A) and 2-protein (B) complexes. The on-resonance STD NMR spectrum has approximately 40-fold in case of **1** and 200-fold lower in case of **2**, lower intensity compared to the reference spectrum.

present in the binding mode of the protein. Thus, both components of the complexes, aspirin or o-hydroxy-benzoic acid and triphenylphosphine have binding affinity 10^{-3}–10^{-8} M at LOX receptor [16]. This experiment provides direct evidence for the binding affinity of the complexes with LOX and supports experimental results reported above.

2.5. Computational studies – molecular docking

In order to investigate further the binding of complexes **1** and **2** towards LOX activity, theoretical docking studies were performed. Complexes are docked into different pockets indicating different interaction relationships towards the enzyme inhibition.

The complex **1** binds into the space defined by the larger hydrophobic pocket of LOX of approximate volume of 573 Å^3 and a smaller one of 160 Å^3. Relevant amino acids are: Ala76, Arg767, Asn128, Asn769, Asp760, Asp768, Gln766, Glu78, Glu761, Gly75, Gly765, His771, Leu74, Lys110, Met15, Phe782, Pro770, Thr73, Trp772 and Val762. Hydrogen bonding interaction appears between the acetyl-O and the N atom of Arg767. The lowest binding energy upon EI (E = enzyme, I = inhibitor) complex formation, was found to be -55.7 kJ/mol. On the contrary, 2 resides into a pocket of

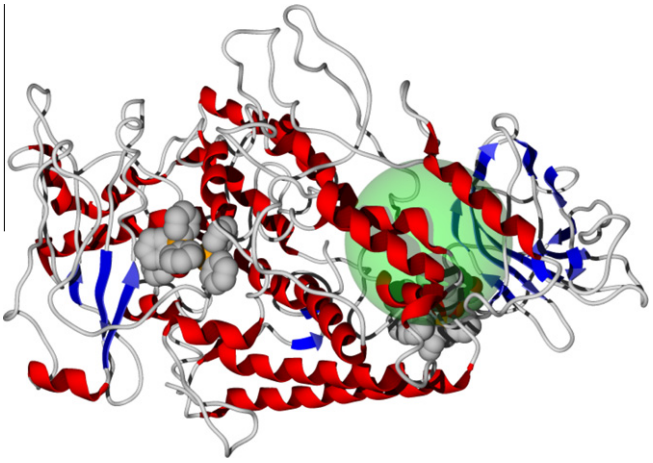

Fig. 6. The binding sites for EI complexes (and ESI in the case of **1**). The sphere indicates the active site as this was resulted from our previous work [10f].

256 Å^3 defined by Ala569, Arg360, Arg588, Asn355, Asn502, Asn573, Asp408, Asp411, Asp578, Asp584, Cys357, Gln579, Ile359, Ile412, Leu407, Leu501, Lys587, Met406, Met497, Ser498, Trp574, Tyr409, Tyr493, Tyr571, Val358, Val570 and Val575. Protein–ligand hydrogen bonds are formed between the coordinated O atoms and N atoms of Arg360 and O atom of Tyr493. The binding energy for the stable EI complex formation was found to be −76.7 kJ/mol. To this value, hydrogen bonds contribute by 7% while significant contribution stems from the ligand steric interactions. The binding sites for EI complexes are shown in Fig. 6, while the sphere indicates the active site of reversible inhibitors as this was resulted from our previous work [10f]. It is shown that **1** binds into LOX in the same pocket that all reversible inhibitors docked, while **2**, in different site away.

The crystal structure of LOX (E) does not include the substrate (linoleic acid, S) as the co-crystallized cofactor and therefore to test the binding affinity we have evaluated the binding energy when the ES complex is formed to be −100.2 kJ/mol. Linoleic acid docks exactly at the larger binding cavity of the protein which is the preferred activity site as shown previously by our group [10b,e,f]. In the case of **1**, when the ESI (enzyme:substrate:inhibitor) complex is formed, the results are ambiguous concerning the exact binding pocket. The calculation outcome showed that the variation of the scoring energies among different sites is minimal. The stability, as this is reflected by steric and hydrogen bonding factors is comparable with the EI complex and constantly lower than that of ES by almost 40%. The complex **2** resides into the same pocket albeit having a different orientation which adds 32 kJ/mol to the stability of the ESI complex compared to the EI case due to increased steric interactions. As a result, this compound acts as inhibitor which always binds at a site away from the substrate binding site, causing a reduction in the catalytic rate which may eventually lead to cell death.

3. Conclusions

Since the relationship between inflammation and carcinogenesis has been examined in numerous biochemical studies [1a,17], the synthesis of new metal complexes with anti-inflamatory drugs, such as aspirin, is one of the strategies employed for the development of new metallotherapeutics. Thus, two new mixed ligand silver(I) complex of formula {[Ag(tpp)$_3$(asp)](dmf)} (**1**) and [Ag(tpp)$_2$(o-Hbza)] (**2**) were synthesized and characterized. The geometry around the silver(I) ion is tetrahedral in both complexes. Complexes **1** and **2** were tested for their *in vitro* cell growth proliferation activity with IC$_{50}$ values 1.5 and 1.6 μM (**1**) and 1.6 and 2.5 μM (**2**) against LMS and MCF-7 cells, respectively. These values indicate stronger activity than the corresponding of cisplatin [10a,14a]. Silver(I) complexes of formula {[AgCl(tptp)$_3$] (0.5 H_2O)}, [AgI(tptp)$_3$] (tptp = tris(p-tolyl)phosphine) or [AgCl(cmbzt)(tptp)$_2$] (cmbzt = 5 chloro-2-mercapto-benzimidazole) with tetrahedral geometry around the metal center, on the other hand, also exhibit strong cytostatic activity against LMS cells with IC$_{50}$ values 0.8 ± 0.08, 1.5 ± 0.06 and 8 ± 0.39 μM, respectively (Table 1) [5]. Flow cytometry assay (*in vitro*) show that when LMS cells are treated with **1** at concentration of 1.5 μM, 44.1% of cells undergo programmed cell death (apoptosis), while when they were treated with **2** at 1.6 μM 29.6% were apoptotic. However, 62.4% of LMS cell were apoptotic when they treated with [AgCl(cmbzt)(tptp)$_2$] complex at 15 μM [5]. This indicates that **1** and **2** likely acts though apoptosis. This is further supported by the high LOX inhibitory activity caused by these complexes with IC$_{50}$ values 7.2 (**1**) and 2.3 (**2**) μM, respectively, since LOX inhibition, is found to induce apoptosis [9c]. STD ^{1}H NMR studies also show that **1** has high binding affinity to LOX.

4. Experimental

4.1. Materials and instruments

All reagents were purchased from commercial sources and used as received. Solvents used were of reagent grade, while acetylsalicylic acid and triphenylphosphine (Sigma–Aldrich, Merck) were used without further purification. Melting points were measured in open tubes with a Stuart scientific apparatus and are uncorrected. Infra-red spectra in the region of 4000–370 cm^{-1} were obtained in KBr disks, with a Perkin–Elmer Spectrum GX FT-IR spectrophotometer. The ^{1}H, ^{13}C NMR spectra were recorded on a Bruker AC250 MHz FT-NMR instrument in DMSO-d_6 solution. Chemical shifts δ are reported in ppm using ^{1}H TMS as an internal reference. Thermal studies were carried out on a Shimadzu DTG-60 simultaneous DTA-TG apparatus, under N_2 flow (50 cm^3 min^{-1}) with a heating rate of 10 °C min^{-1}. A Jasco UV/Vis/NIR V570 series spectrophotometer was used to obtain electronic absorption spectra. Conductivity measurements were carried out at 293 K in DMSO solutions with a WTF LF-91 conductivity meter.

4.2. Synthesis and crystallization of *1* and *2*

A solution of 0.5 mmol ligand (o-acetyl-salicylic acid (aspH) (0.090 g) and o-hydroxy-benzoic acid (o-HbzaH) (0.069 g)) in water (5 cm^3) was added dropwise to a stirred solution of 0.5 mmol silver(I) nitrate (0.085 g) in water (5 cm^3) at room temperature and a clear solution obtained. The resulted solution was treated by 0.5 cm^3 NaOH 1 N and a white powder precipitated immediately which was filtered off. 0.057 g (1) or 0.040 g (2) of the resulting powder was dissolved in DMF (10 ml) and 0.132 g triphenylphospine (0.5 mmol) was added. The mixture was stirred for 30 min at 50 °C and the clear solution was kept in darkness. White crystals of **1** and **2** suitable for X-ray analysis were grown from slow evaporation of the solution after 2 days.

*Compound **1**:* White crystal, Yield: 0.135 g; melting point: 162–165 °C. Elemental analysis, Anal. Calc. for $C_{66}H_{55}AgN_1O_5P_3$: C: 69.36; H: 4.85; N, 1.23. Found: C: 69.23; H: 4.80; N: 1.33%. IR (cm^{-1}), (KBr): 3052 m, 1747s, 1665s, 1594vs, 1479vs,1435vs, 1092vs,743vs, 694vs, 512vs, 494vs; Far-IR (cm^{-1}), (polyethylene): 277vs, 254s, 242m, 225m, 202s; ^{1}H-NMR (ppm) in DMSO-d_6: 7.47–7.23 ppm (m, H(Caromatic), 2.87 and 2.71 ppm (s, H(CH_3– of DMF)), 2.07 ppm (s, H(CH_3– of acetyl group)); MS *m*/*z*: 632.9

$[Ag(tpp)_2]^+$, 368.8 $[Ag(tpp)]^+$, 261.9 $[tpp]^+$, UV–Vis (DMSO): λ_{max} = 259 nm (log ε = 4.6).

Compound ***2****:* White crystal, Yield: 0.174 g; melting point: 189–191 °C. Elemental analysis, Anal. Calc. for $C_{43}H_{35}AgO_3P_2$: C: 67.12; H: 4.58. Found: C: 67.43; H: 4.71%. IR (cm^{-1}), (KBr): 3052m, 1619vs, 1591vs, 1562vs, 1457vs, 1437vs, 1352vs, 1305vs, 511vs, 434m; Far-IR (cm^{-1}), (polyethylene): 279vs, 253s, 247s; ^{1}H NMR (ppm) in DMSO-d_6: 15.88 ppm (br, H(HO), 7.68–6.55 ppm ((m, H(Caromatic); MS *m*/*z*: 632.9 $[Ag(tpp)_2]^+$, 368.8 $[Ag(tpp)]^+$, 261.9 $[tpp]^+$, UV–Vis (DMSO): λ_{max} = 261 nm (log ε = 4.6).

4.3. X-ray structure determination

Data for **1** studied were collected by the θ–2θ scan technique in the θ range 5.11–13.96° (**1**) on a Bruker P4 diffractometer, while intensity data for the crystals of **2** and **3** were collected by the θ–2θ scan technique in the θ range 2.82–28.93° (**2**), 2.88–32.54° (**3**), on an Oxford Diffraction CCD instrument [18a], using graphite-monochromated Mo Kα (λ = 0.71073 Å) radiation. Cell parameters were determined by least-squares fit from 32 reflections in the range. The structures were solved with direct methods with SHELXS-97 [18b] and refined by full-matrix least-squares procedures on F^2 with SHELXL-97 [18c]. All non-hydrogen atoms were refined anisotropically, hydrogen atoms were located at calculated positions (C–H = 0.93–0.97 Å) and refined as a 'riding model'.

Compound ***1****:* $C_{66}H_{59}AgN_1O_5P_3$: MW = 1146.9, triclinic, space group $P\bar{1}$, a = 12.724(2) Å, b = 13.662(3) Å, c = 19.746(5) Å, α = 95.98(2)°, β = 102.66(2)°, γ = 117.490(10)°, V = 2886.1(11) Å^3, Z = 2, T = 293(2), $\rho_{(calc)}$ = 1.309 g cm^{-3}, μ = 0.481 mm^{-1}, F(0 0 0) = 1174. The refinement converged to final R [for 6304 reflections with $I > 2\sigma(I)$] = 0.0945. wR = 0.3023 (all 9931).

Compound ***2****:* $C_{43}H_{35}AgO_3P_2$: MW = 769.5, monoclinic, space group $P2_1/n$, a = 8.909(5) Å, b = 19.527(5) Å, c = 20.754(5) Å, β = 97.229(5)°, V = 3582(2) Å^3, Z = 4, T = 293(2), $\rho_{(calc)}$ = 1.427 g cm^{-3}, μ = 0.692 mm^{-1}, F(0 0 0) = 1576. The refinement converged to final R [for 8935 reflections with $I > 2\sigma(I)$] = 0.0226. wR = 0.0571 (all 54953).

Compound ***3***: $C_7H_5AgO_3$: MW = 245.0, monoclinic, space group $P2_1/c$, a = 7.4030 Å, b = 8.7010 Å, c = 10.5450 Å, β = 107.2660°, V = 646.96(3) Å^3, Z = 4, T = 293(2), $\rho_{(calc)}$ = 2.505 g cm^{-3}, μ = 3.055 mm^{-1}, F(0 0 0) = 468. The refinement converged to final R [for 2338 reflections with $I > 2\sigma(I)$] = 0.0164. wR = 0.0409 (all 9931).

4.4. Biological tests

4.4.1. MTT assay

Cell growth inhibition was analyzed using the 3-(4,5-dimethylthiazol-2-yl)-2,5-diphenyltetrazolium bromide (MTT) assay. LMS, MCF-7 and MRC-5 cells cultured on 96-well plates and maintained in DMEM with 10% fetal calf serum (FCS), incubated at 37 °C, 5% CO_2. A DMSO solution (0.008–0.020% v/v DMSO in DMEM for the complexes and 0.01–0.1% v/v DMSO in DMEM for the ligands) containing different concentrations of the compounds tested (0.5–20 μM for the complexes and 10–400 μM for the ligands) was then added. After incubation for 48 h, 50 μl of MTT was added in each well from a stock solution (3 mg/ml), and incubated for an additional 3 h. Blue formazans were eluted from cells by adding 200 μl of DMSO under gentle shaking and absorbance was determined at 550 nm (subtract background absorbance measured at 690 nm) using a microplate spectrophotometer (Diagnostics Pasteur LP 400). Three to five independent experiments were performed for each compound.

4.4.2. Flow cytometry

LMS cells were seeded onto six-well plates at a density of 6×10^4 cells per well and incubated for 24 h before the experiment. Cells were washed with PBS, treated with media containing various concentrations of **1** and **2** (1.5 and 1.9 μM (**1**) and 1.6 and 2.3 μM (**2**)) in DMSO (0.008–0.020% v/v) and incubated for 48 h. Supernatants and cells collected were centrifuged and cell pellets were suspended in calcium buffer 1× at a rate 10^5 cells/100 μl. Cells were stained with Annexin (BD 556420) and Propidium Iodide (Sigma P4864) in a dark room for 15 min. DNA content was determined on a FACScan flow cytometer (Partec ML, Partec GmbH, Germany). Percentage of apoptotic, necrotic and decompensate cells were calculated over all viable cells (100%). Two replicates were performed for each complex.

4.5. Study of lipoxygenase inhibition mechanism

These studies were performed as previously reported [10f,15].

4.6. Saturation Transfer Difference ^{1}H NMR experiments

NMR samples for the STD experiments were prepared in 99.9% D_2O buffer containing 20 mM TRIS (98% D_{11}), 7 mM $(ND_4)_2SO_4$ (98% D_8), 3.5 mM $MgCl_2$ and 0.3 mM DTT (98% D_{10}), pD 9. Ligand concentration was 0.4 mM and the protein concentration was 0.004 mM resulting in protein–ligand ratio of 1:100.

The STD NMR experiments [16] were recorded on Varian Direct-Drive 800 MHz spectrometer equipped with a Cryoprobe probe with spectral width of 8117 Hz, 8192 complex data points, and 5000 scans at 30 °C. Relaxation delay was set to 9.6 s according to the longest ^{1}H T_1 relaxation time of the ligands. Selective on-resonance irradiation frequency was set to 0.32 ppm with saturation time of 0.4 s. Selective pulse consisted of a train of 50 ms Gauss-shaped pulses separated by a 1 ms delay. Off-resonance irradiation frequency for the reference spectrum was applied at 30 ppm. Water suppression was achieved with excitation sculpting [19]. Spectra were zero filled twice and line broadening function of 1 Hz was applied.

5. Computational details

Molecular docking was performed with the grid based version of the MOLDOCK scoring function [20] as this is implemented in MOLEGRO VIRTUAL DOCKER software (www.molegro.com). Flexible torsions were assigned automatically and no constrains were applied; geometry optimizations based on the X-ray structures of the complexes were carried out using the Forcite module (www.accelrys.com) to confirm that no significant divergence in the conformations of the complexes exist due to crystal packing effects. The universal forcefield, which is parameterized for the full periodic table, was adopted for the minimizations. The three dimensional coordinates of LOX (pdb ID: 1F8N) were obtained from the Protein Data Bank. (www.rcsb.org/pdb) and solvent molecules within the protein structure were removed prior to the docking procedure. The docking space was adequate to cover an extensive domain and was defined as a sphere of 34 Å in diameter with its origin at the center of the enzyme. Due to the stochastic nature of the ligand–protein docking search algorithm, 15 runs were conducted and ten poses were retained for each ligand. The docked derivatives were scored and reranked using the "reranking score" scheme which is a weighted linear combination of the intermolecular interactions (steric, Van der Waals, hydrogen bonding, electrostatic) between the ligand and the protein, and intramolecular interactions (torsional, sp^2–sp^2, steric, Van der Waals, hydrogen bonding, electrostatic) of the ligand. Steric interactions between the ligands and the protein or the cofactor were assigned and calculated using the piecewise linear potential (PLP) Energy

minimization of each pose with regard to its score energy and its orientation was taken into account for the final ranking.

Acknowledgments

M.P. acknowledges the Ministry of Education of Greece for the financial support (decision number 94975/I/04.08.2009). The NMR studies were supported by EN-FIST Centre of Excellence (Dunajska 156, SI-1000 Ljubljana, Slovenia) and Ministry of Higher Education, Science and Technology of Slovenia. T.M. is a recipient of a grant by East-NMR program.

Appendix A. Supplementary material

CCDC 776894, 791214 and 791213 contain the supplementary crystallographic data for compounds **1**, **2** and **3**, respectively. These data can be obtained free of charge from The Cambridge Crystallographic Data Centre via www.ccdc.cam.ac.uk/data_request/cif. Supplementary data associated with this article can be found, in the online version, at doi:10.1016/j.ica.2011.04.032.

References

[1] (a) S. Zha, V. Yegnasubramanian, W.G. Nelsona, W.B. Isaacs, A.M. De Marzo, Cancer Lett. 215 (2004) 1;
(b) J.E.F. Raynolds (Ed.), Martidale the Extra Pharmacopoeia, 28th ed., The Pharmaceutical Press, London, 1982.
[2] (a) L.A. Garcia Rodriguez, C. Huerta-Alvarez, Epidemiology 11 (2000) 376;
(b) E.M. Moran, J. Environ. Pathol. Toxicol. Oncol. 21 (2002) 193;
(c) M.J. Thun, S.J. Henley, C. Patrono, J. Natl. Cancer Inst. 94 (2002) 252.
[3] M.A. Abdellah, S.K. Hadjikakou, N. Hadjiliadis, M. Kubicki, T. Bakas, N. Kourkoumelis, Y.V. Simos, S. Karkabounas, M.M. Barsan, I.S. Butler, Bioinorg. Chem. Appl., 2009, doi:10.1155/2009/542979 (Article ID 542979).
[4] H.S. Rosenkranz, S. Rosenkranz, Antimicrob. Agents Chemother. 2 (1972) 373.
[5] L. Kyros, N. Kourkoumelis, M. Kubicki, L. Male, M. Hursthouse, I.I. Verginadis, E. Gouma, S. Karkabounas, K. Charalabopoulos, S.K. Hadjikakou, Bioinorg. Chem. Appl., 2010, doi:10.1155/2010/386860 (Article ID 386860).
[6] (a) S. Zartilas, S.K. Hadjikakou, N. Hadjiliadis, N. Kourkoumelis, L. Kyros, M. Kubicki, M. Baril, I.S. Butler, S. Karkabounas, J. Balzarini, Inorg. Chim. Acta 362 (2009) 1003;
(b) P.C. Zachariadis, S.K. Hadjikakou, N. Hadjiliadis, A. Michaelides, S. Skoulika, J. Balzarini, E. De Clercq, Eur. J. Inorg Chem. (2004) 1420;
(c) S.K. Hadjikakou, I.I. Ozturk, M.N. Xanthopoulou, P.C. Zachariadis, S. Zartilas, S. Karkabounas, N. Hadjiliadis, J. Inorg. Biochem. 102 (2008) 1007.
[7] (a) P. Ochsenbein, M. Bonin, O. Masson, D. Loyaux, G. Chapuis, K.J. Schenk, Angew. Chem., Int. Ed. 43 (2004) 2694;
(b) T. Fujimori, S. Yamada, H. Yasui, H. Sakurai, Y. In, T. Ishida, J. Biol. Inorg. Chem. (JBIC) 10 (2005) 831;
(c) B. Viossat, J.-C. Daran, G. Savouret, G. Morgant, F.T. Greenaway, Nguyen-Huy Dung, V.A. Pham-Tran, J.R.J. Sorenson, J. Inorg. Biochem. 96 (2003) 375;
(d) Z. Ma, B. Moulton, Cryst. Growth Des. 7 (2007) 196;
(e) M.D. Santana, A.A. Lozano, G. Garcia, G. Lopez, J. Perez, Dalton Trans. (2005) 104;
(f) B.D. James, L.M. Kivlighon, B.W. Skelton, A.H. White, Appl. Organomet. Chem. 12 (1998) 13;
(g) H. Vasquez-Arciga, A. Perez-Benitez, A. Alvarez-Hernandez, S. Bernes, M.A. Mendez-Rojas, Acta Crystallogr., Sect. E Struct. Rep. 60 (2004) m1621;
(h) P. Lemoine, B. Viossat, Nguyen Huy Dung, A. Tomas, G. Morgant, F.T. Greenaway, J.R.J. Sorenson, J. Inorg. Biochem. 98 (2004) 1734.
[8] (a) G. Smith, C.H.L. Kennard, T.C.W. Mak, Z. Kristallogr. 184 (1988) 275;
(b) M. Wolcyrz, M. Pasciak, J. Kowalczyk, M. Maciejewski, Z. Kristallogr. 221 (2006) 270.
[9] (a) B. Samuelsson, S.E. Dahlen, J. Lindgren, C.A. Rouzer, C.N. Serhan, Science 237 (1987) 1171;
(b) M.J. Knapp, J.P. Klinman, Biochemistry 42 (2003) 11466;
(c) X.-Z. Ding, C.A. Kuszynski, T.H. El-Metwally, T.E. Adrian, Biochem. Biophys. Res. Commun. 266 (1999) 392;
(d) G.P. Pidgeon, j. Lysaght, S. Krishnamoorthy, J.V. Reynolds, K. O'Byrne, D. Nie, K.V. Honn, Cancer Metastasis Rev. 26 (2007) 503.
[10] (a) K. Lazarou, B. Bednarz, M. Kubicki, I.I. Verginadis, K. Charalabopoulos, N. Kourkoumelis, S.K. Hadjikakou, Inorg. Chim. Acta 363 (2010) 763;
(b) I. Ozturk, S. Filimonova, S.K. Hadjikakou, N. Kourkoumelis, V. Dokorou, M.J. Manos, A.J. Tasiopoulos, M.M. Barsan, I.S. Butler, E.R. Milaeva, J. Balzarini, N. Hadjiliadis, Inorg. Chem. 49 (2010) 488;
(c) K.N. Kouroulis, S.K. Hadjikakou, N. Kourkoumelis, M. Kubicki, L. Male, M. Hursthouse, S. Skoulika, A.K. Metsios, V.Y. Tyurin, A.V. Dolganov, E.R. Milaevag, N. Hadjiliadis, Dalton Trans. (2009) 10446;
(d) I.I. Ozturk, S.K. Hadjikakou, N. Hadjiliadis, N. Kourkoumelis, M. Kubicki, A.J. Tasiopoulos, H. Scleiman, M.M. Barsan, I.S. Butler, J. Balzarini, Inorg. Chem. 48 (2009) 2233;
(e) V.I. Balas, S.K. Hadjikakou, N. Hadjiliadis, N. Kourkoumelis, M.E. Light, M. Hursthouse, A.K.Metsios, S. Karkabounas, Bioinorg. Chem. Appl., 2008, doi:10.1155/2008/654137 (Article ID 654137).;
(f) M.N. Xanthopoulou, S.K. Hadjikakou, N. Hadjiliadis, E.R. Milaeva, J.A. Gracheva, V.Yu. Tyurin, N. Kourkoumelis, K.C. Christoforidis, A.K. Metsios, S. Karkabounas, K. Charalabopoulos, Eur. J. Med. Chem. 43 (2008) 327;
(g) M.N. Xanthopoulou, S.K. Hadjikakou, N. Hadjiliadis, M. Kubicki, S. Skoulika, T. Bakas, M. Baril, I.S. Butler, Inorg. Chem. 46 (2007) 1187;
(h) M.N. Xanthopoulou, S.K. Hadjikakou, N. Hadjiliadis, M. Schurmann, K. Jurkschat, A. Michaelides, S. Skoulika, T. Bakas, J. Binolis, S. Karkabounas, K. Charalabopoulos, J. Inorg. Biochem. 96 (2003) 425.
[11] (a) R. Noguchi, A. Sugie, Y. Okamoto, A. Hara, K. Nomiya, Bull. Chem. Soc. Jpn. 78 (2005) 1953;
(b) H.M. Hilliard, J.T. Yoke, Inorg. Chem. 5 (1966) 57;
(c) A. Burini, B.R. Pietroni, R. Galassi, G. Valle, S. Calogero, Inorg. Chim. Acta 229 (1995) 299.
[12] (a) P . Rombke, A. Schier, H. Schmidbaur, S. Cronje, H. Raubenheimer, Inorg. Chim. Acta 357 (2004) 235;
(b) W. Shi, L. Zhang, M. Shafaei-Fallah, A. Rothenberger, Z. Anorg. Allg. Chem. 633 (2007) 2431;
(c) Effendy, C. di Nicola, C. Pettinari, A. Pizzabiocca, B.W. Skelton, N. Somers, A.H. White, Inorg. Chim. Acta 359 (2006) 64;
(d) T.S.A. Hor, S.P. Neo, C.S. Tan, T.C.W. Mak, K.W.P. Leung, R-J. Wang, Inorg. Chem. 31 (1992) 4510;
(e) G.A. Bowmaker, Effendy, J.V. Hanna, P.C. Healy, J.C. Reid, C.E.F. Rickard, A.H. White, J. Chem. Soc., Dalton Trans. (2000) 753;
(f) M.-C. Brandys, R.J. Puddephatt, J. Am. Chem. Soc. 124 (2002) 3946.
[13] S.S. Batsanov, Inorg. Mater. 37 (2001) 871.
[14] (a) H.M. Coley, F.H. Labeed, H. Thomas, M.P. Hughes, Biochim. Biophys. Acta 1770 (2007) 601;
(b) N. Shaik, A. Martınez, I. Augustin, H. Giovinazzo, A. Varela-Ramırez, M. Sanau, R.J. Aguilera, M. Conte, Inorg. Chem. 48 (2009) 1577.
[15] M.N. Xanthopoulou, S.K. Hadjikakou, N. Hadjiliadis, M. Kubicki, S. Karkabounas, K. Charalabopoulos, N. Kourkoumelis, T. Bakas, J. Organomet. Chem. 691 (2006) 1780.
[16] M. Mayer, B. Meyer, J. Am. Chem. Soc. 123 (2001) 6108.
[17] (a) G.P. Pidgeon, J. Lysaght, S. Krishnamoorthy, J.V. Reynolds, K. O'Byrne, D. Nie, K.V. Honn, Cancer Metastasis Rev. 26 (2007) 503;
(b) M. Cuendet, J.M. Pezzuto, Drug Metab. Drug Interact. 17 (2000) 109.
[18] (a) Oxford Diffraction, CRYSALIS CCD and CRYSALIS RED, version p171.29.2, Oxford Diffraction Ltd., Abingdon, Oxford, England, 2006.;
(b) G.M. Sheldrick, SHELXS-97 Program for Solution of Crystal Structures, University of Gottingen, Germany, 1997.;
(c) G.M. Sheldrick, SHELXL-97 Program for refinement of Crystal Structures, University of Gottingen, Germany, 1997.
[19] (a) H.L. Hwang, A.J. Shaka, J. Magn. Reson. Ser. A 112 (1995) 275;
(b) C. Dalvit, J. Biomol. NMR 11 (1998) 437.
[20] R. Thomsen, M.H. Christensen, J. Med. Chem. 49 (2006) 3315.